IEEE Open Journal of
Ultrasonics, Ferroelectrics, and Frequency Control

Received 27 October 2022; revised 25 April 2023; accepted 5 June 2023.
Date of publication 9 June 2023; date of current version 21 June 2023.

Digital Object Identifier 10.1109/OJUFFC.2023.3284781

Fiber-Optic Frequency and Timing Transfer Over an Urban Optical Fiber Link

MIHO FUJIEDA[1,2] AND MOTOHIRO KUMAGAI[2]

[1]National Astronomical Observatory of Japan, Mitaka, Tokyo 181-8588, Japan
[2]National Institute of Information and Communications Technology, Koganei, Tokyo 184-8795, Japan
CORRESPONDING AUTHOR: M. FUJIEDA (miho.fujieda@nao.ac.jp)

This work was supported in part by the Japan Science and Technology Agency (JST)-Mirai Program, Japan, under Grant JPMJMI18A1; and in part by the Japan Society for the Promotion of Science (JSPS) KAKENHI, Japan, under Grant JP23K04597.

ABSTRACT We have developed a fiber-optic frequency and timing transfer system. It has been installed to provide timing synchronization between NICT and a distant university site connected by a 58-km urban optical fiber link. The timing signal generated at the remote site is derived from a frequency source that is stabilized using the link, and it is synchronized by a transferred timing marker. A second, separate fiber link confirms a timing synchronization uncertainty of 5.7 ns and a 10-MHz frequency instability of less than $\mathbf{10^{-16}}$ at $\mathbf{10^5}$ s averaging time. We additionally demonstrate a timing marker delivery using a code-based signal, which combines nanosecond-level uncertainty with the simplicity and compactness suitable for a system that can be deployed for synchronization across numerous sites.

INDEX TERMS Frequency transfer, time transfer, optical fibers.

I. INTRODUCTION

SHARING time and frequency signals over a wide area creates an attractive infrastructure for applications like wired and wireless communications, satellite laser ranging, and scientific observations such as very long baseline interferometry (VLBI) and radio telescope arrays in general [1]. Naturally, it is also a key requirement for time and frequency metrology.

GPS-disciplined oscillators (GPS-DO) are a widely used option that can provide a frequency instability at the 10^{-13} level and sub-microsecond synchronization [2], [3]. However, this stability is not sufficient for all applications, and there are increasing concerns over the vulnerability of systems based on Global Navigational Satellite Systems (GNSS) to service interruptions or spoofing and jamming attacks [4]. An alternative is to use a hydrogen maser to provide highly stable frequency and timing signals at each site, but the associated cost is often prohibitive. Additionally, such a system still requires a method for long-distance comparisons for periodic frequency calibration of the masers.

Over the last decades, signal transfer over optical fiber has been established as a solution to surpass the stability and accuracy of GNSS links [5]. Recent work has demonstrated timing signal transfer with compensation of fiber-length variation over dark channels of commercial communications fiber [6], [7], [8] and packet-based methods such as "White Rabbit" [9].

Here, we introduce a similar system that robustly provides accurate time and radio frequency signals at a remote site. Our system replaces the complication of a continuous delay compensation of the timing signal with sporadic accurate measurements of the propagation delay. These measurements synchronize the otherwise autonomous generation of timing signals at the remote site, which derives its stability from the transferred frequency signal. We previously demonstrated a fiber-optic transfer system for a 1-GHz signal [10] in a link that provided frequency transfer over 204 km of urban optical fiber [11] without degradation due to fiber-length variation and sufficient stability of the transferred frequency signal to generate timing signals with a jitter of only a few tens of picoseconds.

To address the need to synchronize these timing signals with the local site, we have now modified the transfer system to enable accurate measurements of the propagation delay. After establishing the signal synchronization at the remote site using an appropriately pre-shifted signal, the stability of the transferred frequency is sufficient to maintain coherence. Over a 58-km urban optical fiber link connecting the National Institute of Information and Communications Technology (NICT) and the University of Tokyo (UT) [12],

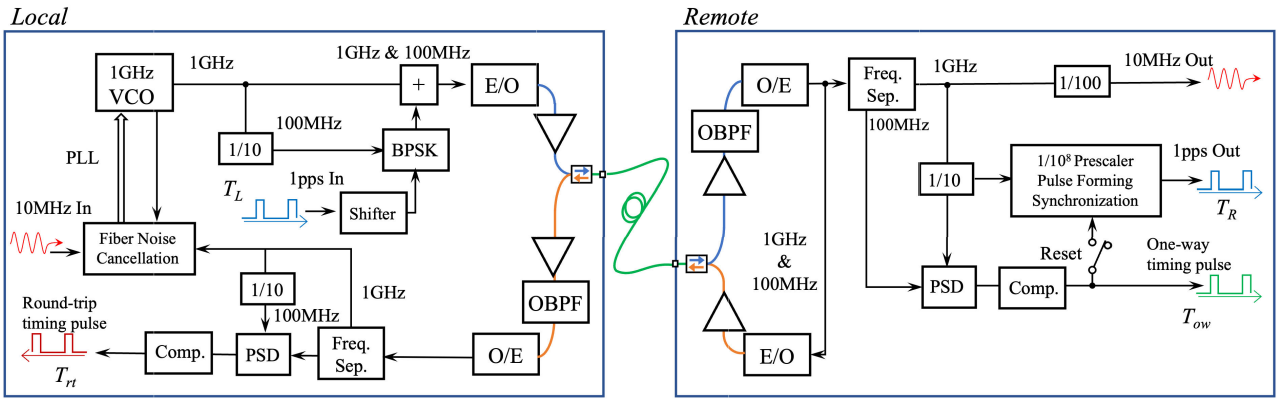

FIGURE 1. Simplified diagram of fiber-optic frequency and timing transfer system. VCO: voltage-controlled oscillator, BPSK: binary phase shift keying, Shifter: pulse shifter with a resolution of 10 nanoseconds, PSD: phase sensitive detection, Comp.: comparator, Freq. Sep.: frequency separator for 100-MHz and 1GHz signals, 1/10 and 1/100: 1/N frequency divider, E/O: Electronic-optical converter, O/E: Optical-electronic converter, and OBPF: optical bandpass filter. Triangle represents a unidirectional Er-doped fiber amplifier (EDFA).

TABLE 1. Uncertainty budget for timing synchronization.

Description	Type A or B	Value [ns]
Systematic delay estimation	B	2.9
Uncertainty of 1-pps restart	A	1.4
Measurement and stability of round-trip delay	A	3.6
Uncertainty due to pulse shifter	B	2.9
Uncertainty of a link to laboratory reference point	A, B	0.5
Total		5.7

Type A effects are expected to vary on repetition, while type B effects likely persist for the entire period of installation.

we evaluate the timing uncertainty of the signals generated at the remote site to be 5.7 nanoseconds (Table 1), and confirm the agreement by an alternative fiber link using modems commonly employed in satellite time and frequency transfer (section IV) [13].

II. EXPERIMENTAL SETUP: FIBER-OPTIC FREQUENCY AND TIMING TRANSFER SYSTEM

A simplified diagram of the fiber-optic frequency and timing transfer system is shown in Fig.1. At the local site, a 1-GHz VCO (voltage-controlled oscillator) compensates phase noise imposed by fiber-length variation as detailed in [11]. The VCO provides a larger control range than widely used variable fiber delay module, improving the system's robustness. An intermediary 100-MHz signal is generated by 1/10 frequency-division of the 1-GHz signal. This is then BPSK (binary phase shift keying)-modulated by a 1-pps signal. The phase modulation realizes a timing marker that indicates the 1-pps timing. A 1550-nm laser source is amplitude-modulated by the sum of the 1 GHz signal and the modulated 100 MHz signal before its single-wavelength output is transmitted via optical fiber.

At the remote site, a portion of the received signal is transmitted back to the local site, where the 1 GHz component is used for fiber noise cancellation. To avoid interference, a laser with different wavelength is used to transmit the returned signal. Spurious reflections are then rejected by optical bandpass filters in front of the optical-electronic converters at both sites.

The remaining signal is separated into 100-MHz and 1-GHz components. The extracted 1-GHz signal serves as the source for the signals supplied to the user: A 10 MHz output signal is generated by 1/100 frequency division, and a 1-pps signal is generated by creating an intermediary 100 MHz signal by 1/10 division, followed by $1/10^8$ frequency-division and pulse shaping.

The timing marker is extracted by coherent detection, through mixing of the received phase-modulated 100 MHz component with the generated intermediary 100 MHz signal. On request, the recovered pulse can be sent to a timing reset mechanism in the 1-pps signal generation, aligning the next pulse with the nearest subsequent zero-crossing of the 100 MHz signal. This function is denoted as "Reset" in Fig.1.

The timing synchronization protocol is performed as follows: The signal returned to the local site also contains the BPSK-modulated 100 MHz signal, such that the timing marker can be extracted by demodulation with a generated intermediary 100 MHz signal like at the remote site. The round-trip propagation delay is then measured by time interval counting. Assuming the forward and backward delays are equal, the one-way propagation delay to the remote site can be pre-compensated by using a pulse shifter at the local site to advance the 1-pps signal by half the round-trip delay. After this adjustment is complete, a timing reset is manually initiated at the remote site to synchronize the timing of the generated 1-pps signal with the delay-compensated timing marker. As the 1-pps signal is generated from the 100 MHz signal, the synchronization allows discrete offsets by 10 nanoseconds. In practical use, the delay compensation also needs to account for the response time of the reset mechanism and for

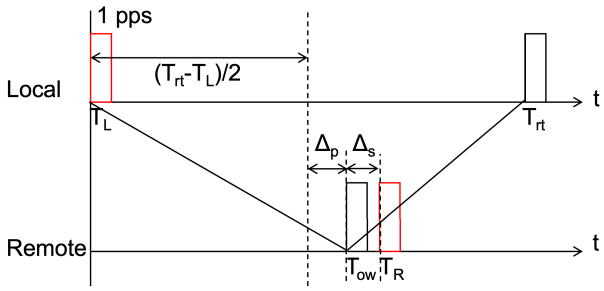

FIGURE 2. **1-pps timing delays. T_L, T_R: time of the reference 1-pps pulse at the local system and time of the realized remote 1-pps pulse. T_{ow}, T_{rt}: time of the one-way and round-trip timing pulses. Δ_S: synchronization offset. Δ_P: difference of the one-way transmission delay from half of the round-trip delay.**

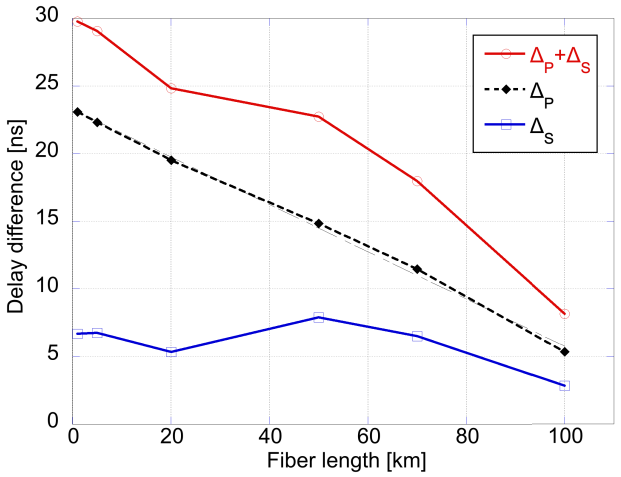

FIGURE 3. **Residual delay differences between the local and remote systems.**

differences in forward and backward delays due to unequal signal paths.

To calibrate these systematic delays, the local and remote terminals are equipped with outputs for the round-trip and one-way timing pulses, respectively. In the following, T_L is the time of the reference 1-pps pulse at the local system, T_R is the time of the realized remote 1-pps pulse, and T_{ow} and T_{rt} are the times of the one-way and round-trip timing pulses, respectively. The round-trip delay is then $T_{rt} - T_L$, and the residual timing difference between the remote and local systems can be considered as

$$T_R - T_L = \frac{(T_{rt} - T_L)}{2} + \Delta_S + \Delta_P \tag{1}$$

before any pre-compensation is applied. Here, Δ_S is the synchronization offset in the remote terminal and Δ_P is the difference of the one-way propagation delay from the expectation of half of the round-trip delay. Fig. 2 shows the relation between 1 pps timings. With both terminals located in the same laboratory and T_R and T_{ow} measured against the same reference signal,

$$\Delta_S = T_R - T_{ow} \tag{2}$$

$$\Delta_P = (T_{ow} - T_L) - \frac{(T_{rt} - T_L)}{2} \tag{3}$$

The propagation delay is then varied by inserting fiber spools of different length, after which Δ_S and Δ_P are determined by time-interval counting $(T_R - T_L)$, $(T_{rt} - T_L)$ and $(T_{ow} - T_L)$, as seen in Fig. 2.

A constant level of the optical signal is maintained by adjustments to the gain of the unidirectional amplifiers (EDFA), such that the changing fiber attenuation does not affect the delay variation in the comparator. Δ_P nevertheless shows a clear linear dependence on the fiber length, which may be considered as follows: The fiber-optic transmission of a pulse signal becomes distorted due to chromatic dispersion. Similar phenomena occur here, increasing the rise time of the recovered timing marker and delaying its detection by the comparator. This effect increases with optical fiber length, and thus affects the round-trip signal more than the one-way signal.

We determine a correction according to the fiber length. Assuming negligible errors in the fiber-spool length, the first order fit to Δ_P shows a maximum residual error of -0.44 ns. Therefore, the uncertainty of Δ_P is conservatively set as 0.5 ns. Reshaping the signal at the remote site before transmission back to the local site would be expected to reduce the observed imbalance Δ_P.

Δ_S originates from the delay of the reset mechanism and the 10 ns quantization resulting from realizing the 1-pps from the 100-MHz signal. From the measurement results in Fig. 3, the mean value and its standard error were 6.0 ns and 1.8 ns, respectively. Since all -equally likely- timings of the reset signal in a 10 ns window will result in the selection of the same zero crossing of the 100 MHz signal for the generation of the 1-pps signal, Δ_S forms a uniform distribution. This distribution fundamentally limits the precision of the timing synchronization, and we take the equivalent standard deviation of 2.9 ns to denote the uncertainty of Δ_S, rather than the smaller measured standard error. Taking the root-sum of the squares of the uncertainties of Δ_P and Δ_S, we determine a total uncertainty for the systematic delay of 2.9 ns.

III. FREQUENCY AND TIMING DISSEMINATION OVER TOKYO OPTICAL FIBER LINK

The 58-km optical fiber link connecting the Koganei headquarter of NICT and the Hongo campus of UT by way of Otemachi [12] has an optical signal loss of -30 dB. Before starting timing and frequency dissemination to UT, the instability of the transfer was measured over the round-trip link NICT-Otemachi-NICT, with a length of 90 km and an optical loss of -30 dB.

Fig. 4 shows the transfer instability of the 10 MHz signal and 1-pps timing to the remote system. For the 10-MHz signal, the fractional instability is $< 3 \times 10^{-14}$ at $\tau = 10$ s

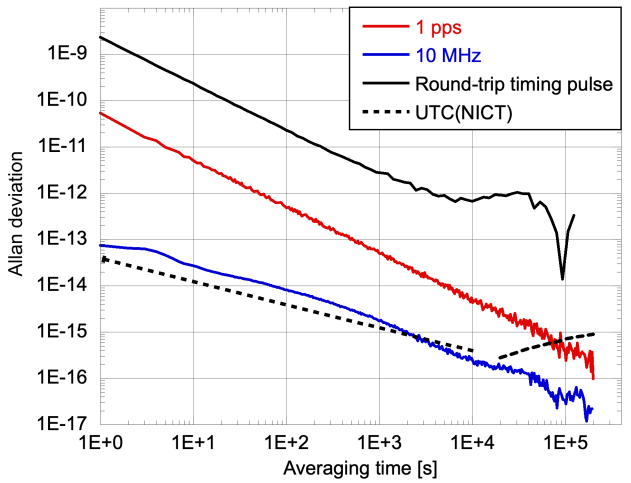

FIGURE 4. Fractional frequency instability of the 10-MHz and 1-pps signals realized at the remote system as well as the round-trip timing pulse over the 90-km round-trip Tokyo fiber link. The measurement bandwidth for the 10 MHz signal is 5 Hz. The dashed line shows a simplified stability model of UTC(NICT), with a frequency instability of $4E-14/(\tau/s)^{1/2}$ for averaging times 1 s $< \tau <$ 10,000 s. As a result of the timescale steering, the frequency instability of UTC(NICT) exceeds that of the fiber link for longer averaging times.

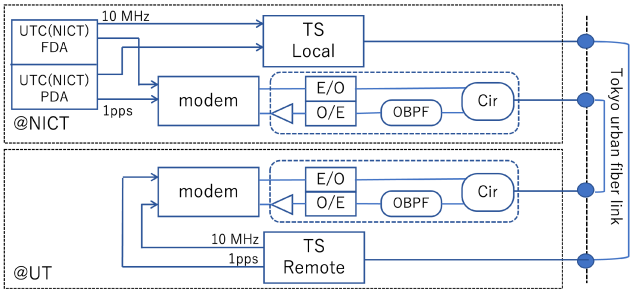

FIGURE 5. Schematic of the timing evaluation. The timing-check system uses a separate fiber connection. FDA: Frequency distribution amplifier, PDA: Pulse distribution amplifier, TS: Transfer system (see Fig. 1), Cir: Circulator, OBPF: Optical bandpass filter.

measurement time and falls to $< 10^{-15}$ at $\tau = 10^4$ s. This is only minimally larger than the instability of UTC(NICT) itself, which in a dead-time-free measurement is dominated by $4 \times 10^{-14}(\tau/s)^{-1/2}$ white frequency noise of the reference hydrogen maser over this range of averaging time [14]. For longer averaging times, the fiber link allows dissemination without further degradation.

After this evaluation, we installed the remote system at UT as shown in Fig. 5 and started the simultaneous dissemination of 10 MHz and 1-pps signals based on UTC(NICT) via the 58-km fiber link. Since the 58-km link introduces less fiber noise than the 90-km round-trip link, we expect an instability of the transferred 10-MHz signal that is no larger than shown in Fig. 4.

The 1-pps signal was synchronized according to the previously described protocol. The systematic delays for the 58-km link were determined as $\Delta_s = 6(2.9)$ ns and $\Delta_p = 13(0.5)$ ns. The pre-compensation matches $T_R - T_L$ calculated according to eq. (1).

Following a command from the local site, the 1-pps signal at the remote site is then set to restart at the zero-crossing point of the 100-MHz signal that follows the detection of the pre-shifted timing marker. The 1-pps restart is affected by the same measurement jitter as the delay determination of the one-way timing pulse, and we therefore assign a statistical uncertainty of 1.4 ns: This is based on the Allan deviation 2×10^{-9} at 1 s averaging time observed in the determination of Δ_s. An additional uncertainty results from the instability of the round-trip delay over the time gap between the measurement of the round-trip delay and the subsequent 1-pps restart after the pre-compensation has been calculated and applied. For a conservative $T_{gap} = 3600$ s, the uncertainty is $\sigma_{gap} = T_{gap} \times \sigma_y(T_{gap})$, with the Allan deviation $\sigma_y(3600s) = 1 \times 10^{-12}$ (see Fig. 4). The round trip delay $(T_{rt} - T_L)$ was determined as 584,075(3.6) ns. The pulse shifter is driven by an internal 100-MHz oscillator, which limits its resolution to 10 ns and thus introduces an additional uncertainty of 2.9 ns for the standard deviation over the uniform distribution across the applicable 10 ns quantization window. Table 1 shows the overall uncertainty budget, which indicates that the 1-pps signal generated at the remote site is synchronized to UTC(NICT) with a total uncertainty of 5.7 ns.

IV. EVALUATION BY FIBER LINK USING TWSTFT MODEMS

Fig. 5 shows a scheme for measuring the time difference over an alternative optical fiber link using modems developed for two-way satellite time and frequency transfer (TWSTFT) [13]. The operation of this timing-check system requires an existing source of 1-pps and 10-MHz signals at each site. The modems employ BPSK signals with a pseudorandom code sequence of 1 Mchip/s over 70 MHz input/output frequency. The head of the code is synchronized to the external 1-pps reference. In TWSTFT, two paired earth stations simultaneously transmit and receive microwave signals through a geostationary satellite and their modems determine the propagation delay from the code and carrier phases [15]. If the systematic delay of the modems is calibrated in advance, the time difference between the two stations can be obtained with nanosecond uncertainty [16]. Here, two distant sites simultaneously transmit and receive optical signals via a shared optical fiber link. The systematic delay in the timing-check system was calibrated with an uncertainty of 2.0 ns by a common-clock reference before the installation at UT.

The timing-check system measured the difference between the time signal transferred to UT as described in the previous sections and the source signal at NICT once per second over a period of 6 days without interruptions. The mean time difference determined by code phase was 4.9 ns, with 0.03 ns

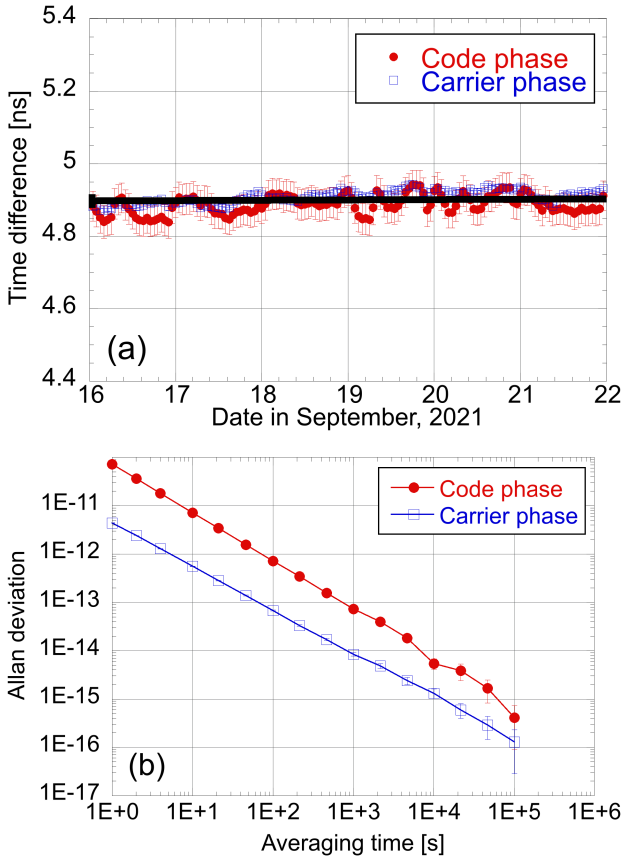

FIGURE 6. **(a) UT-NICT time difference as averages over one hour with error bars indicating the standard deviation of the values contributing to the average. The black line shows the overall mean value of 4.9 ns measured by code phase. Due to the inherent time ambiguity of the carrier phase measurement, an arbitrary constant adjustment value was added for comparison. (b) Frequency instability given as Allan variation.**

standard deviation for the one-hour averages. The overall uncertainty is 2.0 ns, as shown in Table 2. The difference is in good agreement with the uncertainty of the fiber-optic transfer system, evaluated as 5.7 ns in the previous section.

Fig. 6 shows the one-hour averaged time difference of UT-NICT measured by code phase and 70-MHz carrier phases, as well as the corresponding frequency instability. The transferred 10-MHz signal demonstrated an instability of 1.3×10^{-16} at 10^5 s which was marginally larger than that for the time and frequency transfer system as shown in Fig. 4. The increased instability at shorter averaging times indicates noises in the measurement of the 70-MHz carrier phase. The mean frequency difference over 6 days was -6×10^{-17}, surpassing the typical long term instability of UTC(NICT) (see Fig. 4).

V. DEMONSTRATION OF SIMPLE TIMING-MARKER DELIVERY

Nanosecond-level timing is required in applications such as those within the framework of MIFID II financial market

TABLE 2. **Uncertainty budget for evaluation of timing synchronization.**

Description	Type A or B	Value [ns]
Code-phase measurement	A	0.03
Calibration of timing-check system	A, B	2.0
Total		2.0

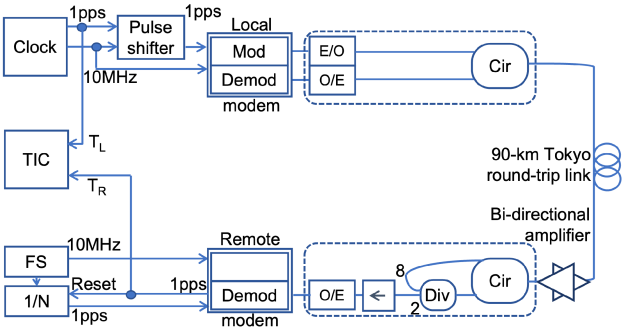

FIGURE 7. **Measurement setup of timing marker delivery over the 90-km Tokyo round-trip link. TIC: Time interval counter, Div: 80%:20% Power splitter, FS: Frequency source, 1/N: Frequency divider.**

regulations [17]. The modem-based approach can be adapted to provide this accuracy.

We have developed a delivery system that embeds the timing marker as the head of the code sequence transmitted over the optical fiber link. This is then detected by a peak search over the correlation integral to generate a 1-pps signal at the remote site. Digital processing avoids the variation of systematic delay with fiber length that is introduced by the analogue demodulation in our time and frequency transfer system. Such use of TWSTFT modems for transmission and reception of timing markers was first reported in ref [18]. Here we demonstrate a further simplified system that avoids the need for a second laser to return the signal and the associated optical filtering. To our knowledge, this is the first use of TWSTFT modems to regenerate and supply a timing marker at the remote site.

Fig. 7 shows the measurement setup of timing marker delivery over the 90-km Tokyo round-trip link. With both terminals located in the same laboratory, the remote terminal is connected to the local timescale for the systematic delay measurement. The BPSK signal with embedded local reference time T_L is transferred via the optical fiber link. At the remote terminal, the received light is split into two portions. The smaller portion is used to recover the BPSK signal. This is demodulated to determine the time information transferred from the local terminal and the arrival time T_{ow} of the marker. T_R is the 1-pps signal regenerated from this time information by the modem.

Meanwhile, the larger portion of the received light is sent back through the fiber link. The modem at the local terminal

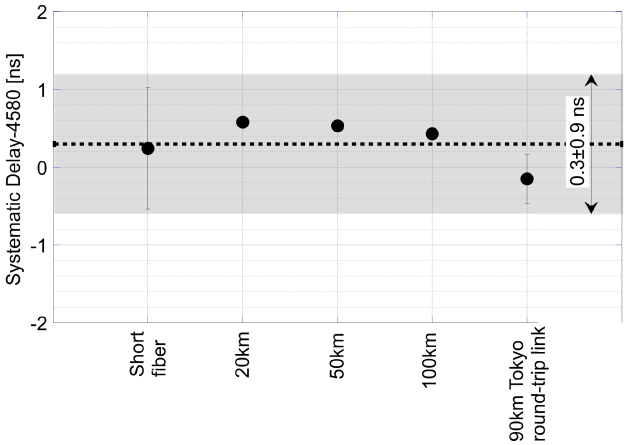

FIGURE 8. **Residual variation of systematic delay Δ measured over different fiber lengths. A constant value of 4580 ns has been subtracted to show the variation more clearly. Error bars show the standard deviation over repeated measurements. No overall trend as a function of fiber length is visible.**

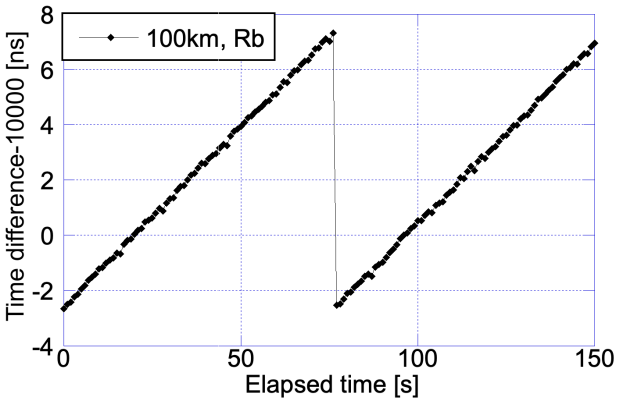

FIGURE 9. **Time interval between the local 1-PPS signal and the 1-PPS signal regenerated by the modem of the remote system, measured in a non-common clock configuration. The additional delay of 10 μs from the modem's adjustable pulse delay has been subtracted.**

then determines the round-trip delay T_{rt} for this returned signal. To compensate for the one-way propagation delay T_{ow}, the transmitted signal is pre-shifted by an opposite amount, which is again estimated by $T_{ow} = T_{rt}/2 + \Delta$, where Δ is a systematic delay. The procedure is essentially identical to that described in section II.

Due to the digital demodulation, the systematic delay Δ is now expected to be independent of fiber length, such that a single calibration is sufficient. To confirm this, we connect both systems via a short fiber with 9-dB optical attenuator, fiber spools of 20 km, 50 km and 100 km length, as well as the 90-km round-trip fiber link. For the last two cases, a bi-directional solid-state optical amplifier is inserted before the remote terminal.

The results are displayed in Fig. 8 and do not show a dependence on fiber length. Over repeated measurements, we find an increased standard deviation of 0.8 ns for the short fiber connection. We attribute this to insufficient temporal separation of spurious reflection signals from e.g. optical connectors. Over the 90-km Tokyo area fiber round-trip, the peaks in the correlation signals representing reflected components become well separated and weakened, and the modem can identify the largest correlation peak and determine its delay with a standard deviation of 0.3 ns.

Next, the remote system was connected to a Rubidium (Rb) frequency standard as a non-common clock. After pre-compensating for half of the round-trip propagation delay over 100 km of spooled fiber, the time difference $(T_R - T_L)$ was measured by time interval counting as shown in Fig. 9. An additional delay of exactly 10 μs was introduced here by using the modem's functionality to output a timing pulse at a specified delay, which is constrained by signal processing to be no smaller than 9 μs. The timing jitter of T_R was approximately 60 ps, dominated by the jitter of the internal oscillator in the modem. The measurement shows a sawtooth pattern with a slope equivalent to a frequency difference of 0.13 mHz between the Rb clock and the local reference. This results from the modem's 100 MHz sampling clock, which only permits adjustment of the generated 1-pps signal in 10 ns increments. The timing remains within ±5 ns of the expected value, except for a small additional delay we attribute to cable length differences in the connection to the phase comparator.

We demonstrated the timing-marker delivery via a code sequence using TWSTFT modems. The digital construction of the marker makes the systematic delay not only independent of the fiber-link length but also repeatable. Furthermore, the narrow-spacing correlation method employed by the modems successfully distinguishes the return signal of the remote terminal from spurious reflections, eliminating the need for re-transmission by a laser of different wavelength. We believe that this concept, with its reduced number of components, is suitable for the mass synchronization of sites as required in applications such as a large-scale antenna array. The number of antenna exceeds 100 in the Square Kilometer Array (SKA) [19], and 200 in the next-generation Very Large Array (ngVLA) [20], [21]. The frequency transfer systems developed for these projects are devoted to higher frequencies such as 8 GHz [22]. Our system can help address their demands for a stand-alone simple and cost-effective timing transfer with low demand on power consumption, dimensions, weight, and maintenance.

Although the delay of the timing marker is not actively stabilized and the arrival time at the remote site changes with the fiber-length variation, timing synchronization to better than 10 ns can be achieved if the compensation protocol is repeated as necessary and without excessive time gap after measuring the round-trip delay.

As shown in Fig. 9, the realized timing is now limited by the sampling clock of the modem. The demonstrated transfer uncertainty is already below the overall system uncertainty target of 10 ns [21], and it seems possible to reach the 2 ns

goal for individual timing links with the implementation of a higher sampling clock or fine adjustment of the 1-pps timing generation.

VI. CONCLUSION

We have developed a fiber-optic frequency and timing transfer system that simultaneous provides 10-MHz and 1-pps signals to the remote site via optical fiber link. We deployed the system to disseminate the UTC(NICT) signal over a 58-km urban optical-fiber link to the University of Tokyo. After calibration of the systematic delay and measurement of the propagation delay, the uncertainty of 5.7 ns was confirmed using an alternative optical fiber link. The system has now continuously provided frequency and timing signals over one and half years, with no loss of timing synchronization except during the maintenance of the optical fiber link.

Furthermore, we demonstrated a new concept of timing marker transfer that uses a TWSTFT modem to directly generate a synchronized 1-pps signal at the remote site. This promises nanosecond-level accuracy with a significantly simplified system and great potential for cost-effective mass-synchronization across sites in ''Beyond 5G'' telecommunication as well as radio astronomy.

ACKNOWLEDGMENT

The authors gratefully acknowledge N. Nemitz from NICT for the helpful discussion and comments on the manuscript. They are also grateful to the provision of JGN optical test bed and the supports by the members. They would like to thank S. Okaba and I. Ushijima from UT for their technical supports on the system installation and T. Gotoh from NICT and H. Kiuchi from NAOJ for the technical discussions. They would also like to thank F. Abe from Spectra Company for the kind supports regarding the modem.

REFERENCES

[1] H. Kimball, ''Handbook selection and use of precise frequency and time systems,'' Int. Telecommun. Union, ITU, Sales Marketing Service, Geneva, Switzerland, Tech. Rep., 1997. [Online]. Available: https://www.itu.int/dms_pub/itu-r/opb/hdb/R-HDB-31-1997-PDF-E.pdf

[2] M. A. Lombardi, ''Evaluating the frequency and time uncertainty of GPS disciplined oscillators and clocks,'' *NCSLI Measure J. Meas. Sci.*, vol. 11, nos. 3–4, pp. 30–44, 2016.

[3] D. Piester, A. Bauch, E. Peik, T. Polewka, E. Staliuniene, and K. Teichel, ''An uncertainty study on traceable frequency and time with disciplined oscillators for metrology and financial sectors,'' in *Proc. Joint Conf. IEEE Int. Freq. Control Symp. Eur. Freq. Time Forum (EFTF/IFC)*, vol. 50, Apr. 2019, pp. 1–4.

[4] T. Humphreys et al., ''Assessing the spoofing threat: Development of a portable GPS civilian spoofer,'' in *Proc. 21st Int. Tech. Meeting Satell. Division Inst. Navigat., ION GNSS*, vol. 2, 2008, pp. 1198–1209.

[5] S. Droste et al., ''Optical-frequency transfer over a single-span 1840 km fiber link,'' *Phys. Rev. Lett.*, vol. 111, no. 11, Sep. 2013, Art. no. 110801.

[6] F. Zuo, Q. Li, K. Xie, L. Hu, J. Chen, and G. Wu, ''Fiber-optic joint time and frequency transmission with enhanced time precision,'' *Opt. Lett.*, vol. 47, nos. 4–15, pp. 1005–1008, 2022.

[7] P. Krehlik, H. Schnatz, and L. Sliwczynski, ''A hybrid solution for simultaneous transfer of ultrastable optical frequency, RF frequency, and UTC time-tags over optical fiber,'' *IEEE Trans. Ultrason., Ferroelectr., Freq. Control*, vol. 64, no. 12, pp. 1884–1890, Dec. 2017.

[8] G. Wu, L. Hu, H. Zhang, and J. Chen, ''High-precision two-way optic-fiber time transfer using an improved time code,'' *Rev. Sci. Instrum.*, vol. 85, no. 11, Nov. 2014, Art. no. 114701.

[9] E. F. Dierikx et al., ''White rabbit precision time protocol on long-distance fiber links,'' *IEEE Trans. Ultrason., Ferroelectr., Freq. Control*, vol. 63, no. 7, pp. 945–952, Jul. 2016.

[10] M. Kumagai, M. Fujieda, S. Nagano, and M. Hosokawa, ''Stable radio frequency transfer in 114 km urban optical fiber link,'' *Opt. Lett.*, vol. 34, no. 19, pp. 2949–2951, 2009.

[11] M. Fujieda, M. Kumagai, and S. Nagano, ''Coherent microwave transfer over a 204-km telecom fiber link by a cascaded system,'' *IEEE Trans. Ultrason., Ferroelectr., Freq. Control*, vol. 57, no. 1, pp. 168–174, Jan. 2010.

[12] *JGN Optical Testbed*. [Online]. Available: https://testbed.nict.go.jp/jgn/english/index.html

[13] M. Fujieda, R. Tabuchi, and T. Gotoh, ''Development of a new digital TWSTFT modem,'' *Int. J. Elect. Eng.*, vol. 27, no. 4, pp. 141–145, 2020.

[14] N. Nemitz et al., ''Absolute frequency of ^{87}Sr at 1.8×10^{-16} uncertainty by reference to remote primary frequency standards,'' *Metrologia*, vol. 58, no. 2, Apr. 2021, Art. no. 025006.

[15] D. Kirchner, ''Two-way satellite time and frequency transfer (TWSTFT): Principle, implementation, and current performance,'' in *Review of Radio Sciences*. London, U.K.: Oxford Univ. Press, 1999, pp. 27–44.

[16] D. Piester, A. Bauch, L. Breakiron, D. Matsakis, B. Blanzano, and O. Koudelka, ''Time transfer with nanosecond accuracy for the realization of international atomic time,'' *Metrologia*, vol. 45, no. 2, pp. 185–198, Apr. 2008.

[17] ''Guidelines on transaction reporting, order record keeping and clock synchronisation under MIFID II,'' Eur. Securities Market Authority (ESMA), Paris, France, Tech. Rep. ESMA/2016/1452, Aug. 2017.

[18] M. Rost, D. Piester, W. Yang, T. Feldmann, T. Wübbena, and A. Bauch, ''Time transfer through optical fibres over a distance of 73 km with an uncertainty below 100 ps,'' *Metrologia*, vol. 49, no. 6, pp. 772–778, Dec. 2012.

[19] P. Diamond. (2020). *SKA Phase 1 Executive Summary*. [Online]. Available: https://www.skatelescope.org/key-

[20] R. Selina et al., ''The next-generation very large array: A technical overview,'' *Proc. SPIE*, vol. 10700, Jul. 2018, Art. no. 107001O.

[21] W. Shillue. (2019). *Local Oscillator Reference and Timing Design Description*. [Online]. Available: https://ngvla.nrao.edu/page/projdoc/

[22] D. R. Gozzard et al., ''Astronomical verification of a stabilized frequency reference transfer system for the square kilometer array,'' *Astronomical J.*, vol. 154, no. 1, p. 9, Jun. 2017.

MIHO FUJIEDA received the Ph.D. degree in physics from Kyoto University, Japan, in 2000. From 2003 to 2022, she was with the National Institute of Information and Communications Technology, Japan, where she was involved in time and frequency transfer via satellite and optical fiber. Since 2022, she has been an Associate Professor with the National Astronomical Observatory of Japan. She is currently involved in time and frequency transfer via optical fiber and optical data communications for large-scale radio astronomy.

MOTOHIRO KUMAGAI received the Ph.D. degree in applied physics from the Tokyo Institute of Technology, Japan, in 2000. In 2000, he joined the Communication Research Laboratory [later National Institute of Information and Communications Technology (NICT)], Japan, where he is currently a Senior Researcher, involved in developments of atomic frequency standards, frequency and timing transfer via optical fiber, and measurement standards at terahertz band.